

D^*K molecular structure of the $D_{s1}(2460)$ meson

Amand Faessler, Thomas Gutsche, Valery E. Lyubovitskij *, Yong-Liang Ma

*Institut für Theoretische Physik, Universität Tübingen,
Auf der Morgenstelle 14, D-72076 Tübingen, Germany*

(Dated: November 4, 2018)

We discuss a possible interpretation of the $D_{s1}(2460)$ meson as a hadronic molecule - a bound state of D^* and K mesons. Using a phenomenological Lagrangian approach we determine the strong $D_{s1} \rightarrow D_s^* \pi^0$ and radiative $D_{s1} \rightarrow D_s \gamma$ decays. In order of magnitude our results for the partial strong and radiative decay widths are consistent with previous calculations.

PACS numbers: 13.25.Ft, 13.40.Hq, 14.40.Lb

Keywords: charm mesons, hadronic molecule, strong and radiative decay, isospin violation

arXiv:0709.3946v2 [hep-ph] 13 Dec 2007

* On leave of absence from the Department of Physics, Tomsk State University, 634050 Tomsk, Russia

I. INTRODUCTION

Nowadays there is strong interest to study newly observed mesons and baryons in the context of a hadronic molecule interpretation (for overview see e.g. Ref. [1]). As stressed for example in Ref. [2] the scalar $D_{s_0}^*(2317)$ and axial $D_{s_1}(2460)$ mesons could be candidates for a scalar DK and a axial D^*K molecule because of a relatively small binding energy of ~ 50 MeV. These states were discovered and confirmed just a few years ago by the Collaborations BABAR at SLAC [3], CLEO at CESR [4] and Belle at KEKB [5]. In the interpretation of these experiments it was suggested that the $D_{s_0}^*(2317)$ and $D_{s_1}(2460)$ mesons are the P -wave charm-strange quark states with spin-parity quantum numbers $J^P = 0^+$ and $J^P = 1^+$, respectively. It is worth noting that the existing experimental information on the properties of the $D_{s_0}^*(2317)$ and $D_{s_1}(2460)$ mesons [6] leaves quite a significant uncertainty in their possible assignment of $J^P = 0^+$ and $J^P = 1^+$ quark-antiquark states.

Strong and radiative decays of the $D_{s_0}^*(2317)$ and $D_{s_1}(2460)$ mesons have been considered using different approaches [7, 8, 9, 10, 11, 12, 13, 14, 15, 16, 17, 18, 19, 20, 21, 22, 23, 24, 25, 26, 27, 28], including their different interpretations as two- and four-quark states and as $D^{(*)}K$ molecules. The range of predictions for the strong and radiative decay widths is from several to a few hundreds keV. In our previous paper [24] we calculated the strong $D_{s_0}^* \rightarrow D_s \pi^0$ and radiative $D_{s_0}^* \rightarrow D_s^* \gamma$ decays using a phenomenological Lagrangian approach [24, 29] for the treatment of the $D_{s_0}^*$ meson as a hadronic molecule - a bound state of D and K mesons. A new feature related to the molecular DK structure of the $D_{s_0}^*(2317)$ meson was that the presence of $u(d)$ quarks in the D and K mesons gives rise to a direct strong isospin-violating transition $D_{s_0}^* \rightarrow D_s \pi^0$ in addition to the decay mechanism induced by $\eta - \pi^0$ mixing as considered previously. We showed that the direct transition dominates over the $\eta - \pi^0$ mixing transition in the $D_{s_0}^* \rightarrow D_s \pi^0$ decay.

In this paper we extend our formalism [24, 29] to the strong and radiative decays of the $D_{s_1}(2460)$ assuming that the latter is a D^*K bound state. As for the case of the $D_{s_0}^*$ state, a composite (molecular) structure of the $D_{s_1}(2460)$ meson is defined by the compositeness condition $Z = 0$ [30, 31, 32] (see also Refs. [24, 29]). This condition implies that the renormalization constant of the hadron wave function is set equal to zero or that the hadron exists as a bound state of its constituents. The compositeness condition was originally applied to the study of the deuteron as a bound state of proton and neutron [30]. Then it was extensively used in low-energy hadron phenomenology as the master equation for the treatment of mesons and baryons as bound states of light and heavy constituent quarks (see e.g. Refs. [31, 32]). Constructing the effective mesonic Lagrangian including D_{s_1} , $D^{(*)}$, $K^{(*)}$ and $D_s^{(*)}$ degrees of freedom we calculate one-loop meson diagrams describing the strong $D_{s_1} \rightarrow D_s^* \pi^0$ and radiative $D_{s_1} \rightarrow D_s \gamma$ decays. A study of two other possible radiative decay modes of the D_{s_1} meson, the transitions $D_{s_1} \rightarrow D_s^* \gamma$ and $D_{s_1} \rightarrow D_{s_0}^* \gamma$, and, also, the extension to the bottom sector ($B_{s_0}^*(5725)$ and $B_{s_1}(5778)$ states) will be done in a forthcoming paper.

In the present manuscript we proceed as follows. First, in Section II we discuss the basic notions of our approach. We discuss the effective mesonic Lagrangian for the treatment of the $D_{s_1}(2460)$ meson as a D^*K bound state. In Section III we consider the matrix elements (Feynman diagrams) describing the strong and radiative decays of the $D_{s_1}(2460)$ meson. We discuss our numerical results and perform a comparison with other theoretical approaches. In Section IV we present a short summary of our results.

II. APPROACH

A. Molecular structure of the $D_{s_1}^\pm(2460)$ meson

In this section we discuss the formalism for the study of the $D_{s_1}^\pm(2460)$ meson as a hadronic molecule, represented by a D^*K bound state. We adopt that the isospin, spin and parity quantum numbers of the $D_{s_1}^\pm(2460)$ are $I(J^P) = 0(1^+)$, while for its mass we take the value $m_{D_{s_1}} = 2.4589$ GeV [6]. Our framework is based on an effective interaction Lagrangian describing the couplings of the $D_{s_1}(2460)$ meson to its constituents:

$$\mathcal{L}_{D_{s_1}}(x) = g_{D_{s_1}} D_{s_1}^{\mu-}(x) \int dy \Phi_{D_{s_1}}(y^2) D_\mu^*(x + w_{KD^*} y) K(x - w_{D^*K} y) + \text{H.c.}, \quad (1)$$

where the doublets of D^* and K mesons are defined as

$$D^* = \begin{pmatrix} D^{*0} \\ D^{*+} \end{pmatrix}, \quad K = \begin{pmatrix} K^+ \\ K^0 \end{pmatrix}. \quad (2)$$

The summation over isospin indices is understood. The molecular structure of the $D_{s_1}^\pm$ states is (we do not consider isospin mixing): $|D_{s_1}^+\rangle = |D^{*+}K^0\rangle + |D^{*0}K^+\rangle$, $|D_{s_1}^-\rangle = |D^{*-}K^0\rangle + |\bar{D}^{*0}K^-\rangle$. The correlation function $\Phi_{D_{s_1}}$

characterizes the finite size of the $D_{s1}(2460)$ meson as a D^*K bound state and depends on the relative Jacobi coordinate y with, in addition, x being the center-of-mass (CM) coordinate. In Eq. (1) we introduced the kinematical parameters $w_{ij} = m_i/(m_i + m_j)$, where m_{D^*} and m_K are the masses of the D^* and K mesons. The Fourier transform of the correlation function reads

$$\Phi_{D_{s1}}(y^2) = \int \frac{d^4p}{(2\pi)^4} e^{-ipy} \tilde{\Phi}_{D_{s1}}(-p^2). \quad (3)$$

A basic requirement for the choice of an explicit form of the correlation function is that it vanishes sufficiently fast in the ultraviolet region of Euclidean space to render the Feynman diagrams ultraviolet finite. We adopt the Gaussian form, $\tilde{\Phi}_{D_{s1}}(p_E^2) \doteq \exp(-p_E^2/\Lambda_{D_{s1}}^2)$, for the vertex function, where p_E is the Euclidean Jacobi momentum. Here, $\Lambda_{D_{s1}}$ is a size parameter, which characterizes the distribution of D^* and K mesons inside the D_{s1} molecule.

The coupling constant $g_{D_{s1}}$ is determined by the compositeness condition [30, 31, 32] (for an application to $D_{s0}^*(2317)$ and $D_{s1}(2460)$ meson properties see Refs. [24, 29].) It implies that the renormalization constant of the hadron wave function is set equal to zero:

$$Z_{D_{s1}} = 1 - \Sigma'_{D_{s1}}(m_{D_{s1}}^2) = 0. \quad (4)$$

Here, $\Sigma'_{D_{s1}}(m_{D_{s1}}^2) = g_{D_{s1}}^2 \Pi'_{D_{s1}}(m_{D_{s1}}^2)$ is the derivative of the transverse part of the mass operator $\Sigma_{D_{s1}}^{\mu\nu}$, conventionally split into the transverse $\Sigma_{D_{s1}}$ and longitudinal $\Sigma_{D_{s1}}^L$ parts as:

$$\Sigma_{D_{s1}}^{\mu\nu}(p) = g_{D_{s1}}^{\mu\nu} \Sigma_{D_{s1}}(p^2) + \frac{p^\mu p^\nu}{p^2} \Sigma_{D_{s1}}^L(p^2), \quad (5)$$

where $g_{D_{s1}}^{\mu\nu} = g^{\mu\nu} - p^\mu p^\nu/p^2$, $g_{D_{s1}}^{\mu\nu} p_\mu = 0$. The mass operator of the D_{s1} meson is described by the diagram of Fig.1.

To clarify the physical meaning of the compositeness condition, we first want to remind the reader that the renormalization constant $Z_{D_{s1}}^{1/2}$ can also be interpreted as the matrix element between the physical and the corresponding bare state. For $Z_{D_{s1}} = 0$ it then follows that the physical state does not contain the bare one and hence is described as a bound state. As a result of the interaction of the D_{s1} meson with its constituents (D^*, K mesons), the D_{s1} meson is dressed, i.e. its mass and its wave function have to be renormalized. The condition $Z_{D_{s1}} = 0$ also effectively excludes the tree-level diagrams involving D_{s1} mesons, because each external leg of the D_{s1} meson is multiplied by the factor $Z_{D_{s1}}^{1/2}$.

Following Eq. (4) the coupling constant $g_{D_{s1}}$ can be expressed in the form:

$$\frac{1}{g_{D_{s1}}^2} = \frac{2}{(4\pi\Lambda_{D_{s1}})^2} \int_0^1 dx \int_0^\infty \frac{d\alpha \alpha P(\alpha, x)}{(1+\alpha)^3} \left[\frac{1}{2\mu_{D^*}^2(1+\alpha)} - \frac{d}{dz} \right] \tilde{\Phi}_{D_{s1}}^2(z) \quad (6)$$

where

$$P(\alpha, x) = \alpha^2 x(1-x) + w_{D^*K}^2 \alpha x + w_{KD^*}^2 \alpha(1-x), \quad z = \mu_{D^*}^2 \alpha x + \mu_K^2 \alpha(1-x) - \frac{P(\alpha, x)}{1+\alpha} \mu_{D_{s1}}^2, \quad \mu_M = \frac{m_M}{\Lambda_{D_{s1}}}. \quad (7)$$

Above expressions are valid for any functional form of the correlation function $\tilde{\Phi}_{D_{s1}}(z)$.

B. Effective Lagrangian for strong and radiative decays of $D_{s1}^\pm(2460)$

In the preceding paper [24] in the analysis of the strong decay $D_{s0}^* \rightarrow D_s \pi^0$ we considered the so-called ‘‘direct’’ diagrams (see Fig.2 in [24]) with π^0 -meson emission from the $D \rightarrow D^*$ and $K \rightarrow K^*$ transitions and the ‘‘indirect’’ diagrams (see Fig.3 in [24]) where a π^0 meson is produced via $\eta - \pi^0$ mixing in the mass term of pseudoscalar mesons in the leading-order $O(p^2)$ Lagrangian of chiral perturbation theory (ChPT) [33, 34]. Note, that the second mechanism based on $\eta - \pi^0$ mixing was mainly considered before in the literature. Originally, it was initiated by the analysis based on the use of chiral Lagrangians [9, 11, 34] where the leading-order, tree-level $D_{s0}^* D_s \pi^0$ coupling can be generated only by virtual η -meson emission. During the last years different approaches have been applied to the $D_{s0}^* \rightarrow D_s \pi^0$ and $D_{s1} \rightarrow D_s \pi^0$ decay properties using the $\eta - \pi^0$ mixing mechanism. In our approach the D_{s0}^* and D_{s1} mesons are considered as DK and D^*K bound states, respectively and, therefore, we have an additional mechanism for generating the $D_{s0}^* \rightarrow D_s \pi^0$ and $D_{s1} \rightarrow D_s \pi^0$ transition due to the direct coupling of $D^{(*)}$ and $K^{(*)}$ mesons to π^0 . One should stress, that the two types of diagrams (‘‘direct’’ and ‘‘mixing’’) can be reduced to modified

pion-emission diagrams performing the diagonalization of the pseudoscalar meson mass term [33]. In particular, after the diagonalization of the mesonic mass term the π^0 and η meson fields are modified by a unitary transformation as [33]:

$$\pi^0 \rightarrow \pi^0 \cos \varepsilon - \eta \sin \varepsilon, \quad \eta \rightarrow \pi^0 \sin \varepsilon + \eta \cos \varepsilon \quad (8)$$

with ε being the $\pi^0 - \eta$ mixing angle fixed as [33]:

$$\tan 2\varepsilon = \frac{\sqrt{3} m_d - m_u}{2 m_s - \hat{m}} \simeq 0.02, \quad \hat{m} = \frac{1}{2}(m_u + m_d) \quad (9)$$

where m_u, m_d, m_s are the current quark masses. As a result of the unitary transformation (8) the ‘‘direct’’ and ‘‘mixing’’ diagrams are combined together in the form of pure pion-coupling diagram with modified flavor structure, i.e. instead of the $\tau_3 \pi^0$ coupling to DD^* or KK^* mesonic pair we have $\pi^0 (\tau_3 \cos \varepsilon + \kappa I \sin \varepsilon)$, where $\kappa = 1/\sqrt{3}$ or $\sqrt{3}$ is the corresponding flavor-algebra factor for DD^* or KK^* coupling, respectively. Below we display the explicit form of the corresponding interaction Lagrangian. The lowest-order diagrams which contribute to the matrix elements of the strong isospin-violating decay $D_{s1} \rightarrow D_s^* \pi^0$ are shown in Fig.2. Note, that in the isospin limit ($m_u = m_d$), the $\eta - \pi^0$ mixing angle vanishes and the masses of the virtual $D^{(*)}$ and $K^{(*)}$ mesons in the loops are degenerate, respectively. As result the pairs of diagrams related to Fig.2(a), 2(b) and Fig.2(c) and 2(d) compensate each other. Therefore, in the calculation of the diagrams of Fig.2 we go beyond the isospin limit and use the physical meson masses.

The diagrams contributing to the radiative decay $D_{s1}^+ \rightarrow D_s^+ \gamma$ are shown in Fig.3. The diagrams of Figs.3(a) and 3(b) are generated by the direct coupling of the charged D^{*+} and K^+ mesons to the electromagnetic field after gauging the free Lagrangians related to these mesons. The diagrams of Figs.3(c) and 3(d) (so-called contact diagrams) are generated after gauging the nonlocal strong Lagrangian (1) describing the coupling of D_{s1} meson to its constituents - D^* and K mesons. The diagrams of Figs.3(e) and 3(f) arise after gauging the strong $D_s D^* K$ interaction Lagrangian containing derivatives acting on the pseudoscalar fields. Finally, the diagrams of Figs.3(g) and 3(h) describe the subprocess, where the D_{s1} first interacts with the electromagnetic field and then converts into the D_s via a $D^* K$ loop. Note that an analogous diagram where the D_{s1} converts into the D_s and then interacts with the electromagnetic field vanishes due to the Lorentz condition for the on-shell axial meson D_{s1} , i.e. $p_\mu \epsilon_{D_{s1}}^\mu(p) = 0$. Details of how to generate the effective couplings of the involved mesons to the electromagnetic field will be discussed later.

After the preliminary discussion of the relevant diagrams, now we are in the position to write down the full effective Lagrangian for the study of the strong and radiative decays of the D_{s1} meson formulated in terms of mesonic degrees of freedom and photons. We follow the procedure discussed in detail in Ref. [24], where we considered the D_{s0}^* meson decay properties. First, we write the Lagrangian \mathcal{L} , which includes the free mesonic parts $\mathcal{L}_{\text{free}}$ and the strong interaction parts \mathcal{L}_{str} :

$$\mathcal{L}(x) = \mathcal{L}_{\text{free}}(x) + \mathcal{L}_{\text{str}}(x), \quad (10)$$

where

$$\begin{aligned} \mathcal{L}_{\text{free}}(x) = & -\frac{1}{2} \vec{\pi}(x) (\square + m_\pi^2) \vec{\pi}(x) + \frac{\delta_\pi}{2} [\pi^0(x)]^2 + D_{s1,\mu}^+(x) (g^{\mu\nu} [\square + m_{D_{s1}}^2] - \partial^\mu \partial^\nu) D_{s1,\nu}^-(x) \\ & - \sum_{P=K,D,D_s} P^\dagger(x) (\square + m_P^2) P(x) + \sum_{P=K,D} \delta_P \bar{P}^0(x) P^0(x) \\ & + \sum_{V=K^*,D^*,D_s^*} V_\mu^\dagger(x) (g^{\mu\nu} [\square + m_V^2] - \partial^\mu \partial^\nu) V_\nu(x) - \sum_{V=K^*,D^*} \delta_V \bar{V}_\mu^0(x) V^{0\mu}(x), \end{aligned} \quad (11)$$

$$\begin{aligned} \mathcal{L}_{\text{str}}(x) = & -\frac{g_{D^* D \pi}}{2\sqrt{2}} D_\mu^{*\dagger}(x) \hat{\pi}_D(x) i \overleftrightarrow{\partial}^\mu D(x) + \frac{g_{K^* K \pi}}{\sqrt{2}} K_\mu^{*\dagger}(x) \hat{\pi}_K(x) i \overleftrightarrow{\partial}^\mu K(x) \\ & + g_{D^* D_s K} D_\mu^*(x) K(x) i \overleftrightarrow{\partial}^\mu D_s^-(x) + g_{D_s^* D K} D_{s,\mu}^*(x) D(x) i \overleftrightarrow{\partial}^\mu K(x) \\ & - ig_{K^* D_s^* D^*} \left[D_s^{*\mu\nu}(x) D_\mu^*(x) K_\nu^*(x) + D^{*\mu\nu}(x) K_\mu^*(x) D_{s,\nu}^*(x) + K^{*\mu\nu}(x) D_{s,\mu}^*(x) D_\nu^*(x) \right] \\ & + g_{D_{s1}} D_{s1}^{\mu-}(x) \int dy \Phi_{D_{s1}}(y^2) D_\mu^*(x + w_{KD^*} y) K(x - w_{D^* K} y) + \text{H.c.}, \end{aligned} \quad (12)$$

where summation over isospin indices is understood, $\square = \partial^\mu \partial_\mu$ and $A \overleftrightarrow{\partial} B \equiv A \partial B - B \partial A$. Here, $\vec{\pi} = (\pi_1, \pi_2, \pi_3)$ is the triplet of pions, $\hat{\pi}_D = \pi_1 \tau_1 + \pi_2 \tau_2 + \pi_3 (\tau_3 \cos \varepsilon + I \sin \varepsilon / \sqrt{3})$, $\hat{\pi}_K = \pi_1 \tau_1 + \pi_2 \tau_2 + \pi_3 (\tau_3 \cos \varepsilon + I \sin \varepsilon \sqrt{3})$, $D^{(*)}$

and $K^{(*)}$ are the doublets of pseudoscalar (vector) mesons, D_s^\pm and $D_s^{*\pm}$ are the pseudoscalar and vector charm-strange mesons, respectively, $V^{*\mu\nu} = \partial^\mu V^{*\nu} - \partial^\nu V^{*\mu}$ is the stress tensor of vector meson field. In our convention the isospin-symmetric meson masses of the isomultiplets m_π, m_P, m_V are identified with the masses of the charged partners. The quantities δ_M are the isospin-breaking parameters which are fixed by the difference of masses squared of the charged and neutral members of the isomultiplets as: $\delta_M = m_{M^\pm}^2 - m_{M^0}^2$ and $m_{M^0} \equiv m_{\bar{M}^0}$. The set of mesonic masses is taken from data [6]. From Eq. (12) it is evident that the couplings of π^0 to D^*D and K^*K mesonic pairs contain two terms - the ‘‘dominant’’ coupling (proportional to $\cos \varepsilon$) and the ‘‘suppressed’’ coupling (proportional to $\sin \varepsilon$). It means that the first coupling survives in the isospin limit, while the second one vanishes. In the context of the ‘‘direct’’ and ‘‘ $\eta - \pi^0$ mixing’’ diagrams considered by us in the preceding paper [24], the first coupling generates the ‘‘direct’’ diagrams of Fig.2 in [24], while the second coupling results in the ‘‘mixing’’ diagrams of Fig.3 in [24].

The free meson propagators are given by the standard expressions

$$i D_M(x-y) = \langle 0|T M(x) M^\dagger(y)|0 \rangle = \int \frac{d^4k}{(2\pi)^4 i} e^{-ik(x-y)} \tilde{D}_M(k) \quad (13)$$

for the scalar (pseudoscalar) fields, where $\tilde{D}_M(k) = (m_M^2 - k^2 - i\epsilon)^{-1}$ and

$$i D_{M^*}^{\mu\nu}(x-y) = \langle 0|T M^{*\mu}(x) M^{*\nu\dagger}(y)|0 \rangle = \int \frac{d^4k}{(2\pi)^4 i} e^{-ik(x-y)} \tilde{D}_{M^*}^{\mu\nu}(k) \quad (14)$$

for the vector (axial) fields, where $\tilde{D}_{M^*}^{\mu\nu}(k) = (-g^{\mu\nu} + k^\mu k^\nu / m_{M^*}^2) (m_{M^*}^2 - k^2 - i\epsilon)^{-1}$.

In Eq. (12) we use the same set of strong coupling constants as used for the decay properties of the D_{s0}^* meson (see details in Ref. [24]). In particular, we have

$$g_{D^*D\pi} = 17.9, \quad g_{K^*K\pi} = 4.61, \quad g_{D^*D_s K} = g_{K^*D_s D} = 2.02, \quad g_{D_s^* D K} = 1.84. \quad (15)$$

The additional three-vector meson coupling $g_{D_s^* D^* K^*}$ is a free parameter in our calculation. It should be of order 1. Finally, we fix the coupling $g_{D_{s1}}$, which is given by Eq. (6) in terms of the adjustable vertex function. Using the Gaussian vertex function we obtain the result that this coupling is quite stable with respect to a variation of the scale parameter $\Lambda_{D_{s1}}$. In particular, varying $\Lambda_{D_{s1}}$ from 1 to 2 GeV, we get a range of values for $g_{D_{s1}}$ from 11.62 to 10.17 GeV. Note, this result is in agreement with prediction of the light-cone QCD sum rules $g_{D_{s1}} = 10.5 \pm 3.5$ GeV [35]. In the following we also test the sensitivity of the decay properties of the D_{s1} meson to the variation of $\Lambda_{D_{s1}}$.

The electromagnetic field is included in the Lagrangian (10) using minimal substitution i.e. each derivative acting on a charged meson field is replaced by the covariant one: $\partial^\mu M^{(*)\pm} \rightarrow (\partial^\mu \mp ieA^\mu) M^{(*)\pm}$. Note, that the strong $D_{s1} D^* K$ interaction Lagrangian should also be modified in order to restore electromagnetic gauge invariance. It proceeds in a way suggested in Ref. [36] and extensively used in Refs. [24, 32]. In particular, each charged constituent meson field (i.e. $D^{*\pm}$ and K^\pm) in $\mathcal{L}_{D_{s1}}$ is multiplied by the gauge field exponential resulting in

$$\begin{aligned} \mathcal{L}_{D_{s1}+\text{em}}(x) &= g_{D_{s1}} D_{s1}^{\mu-}(x) \int dy \Phi_{D_{s1}}(y^2) \left\{ e^{-ieI(x+w_{KD^*}y,x,P)} D_{\mu}^{*+}(x+w_{KD^*}y) K^0(x-w_{D^*K}y) \right. \\ &\quad \left. + D_{\mu}^{*0}(x+w_{KD^*}y) e^{-ieI(x-w_{D^*K}y,x,P)} K^+(x-w_{D^*K}y) \right\} + \text{H.c.} \end{aligned} \quad (16)$$

where

$$I(x, y, P) = \int_y^x dz_\mu A^\mu(z). \quad (17)$$

For the derivative of $I(x, y, P)$ we use the path-independent prescription suggested in [36] which in turn states that the derivative of $I(x, y, P)$ does not depend on the path P originally used in the definition. The nonminimal substitution (16) is therefore completely equivalent to the minimal prescription. We should stress, that in the calculation of the amplitudes of the radiative $D_{s1} \rightarrow D_s \gamma$ decay, in Eq. (16) we only need to keep terms linear in A_μ , that is the four-particle coupling $D_{s1} D^* K \gamma$. Concluding the discussion of the effective Lagrangian we stress that all couplings occurring in the diagrams contributing to the decays $D_{s1} \rightarrow D_s^* \pi^0$ and $D_{s1} \rightarrow D_s \gamma$ are defined and explicitly fixed, except for $g_{D_s^* D^* K^*}$.

III. STRONG AND RADIATIVE DECAYS OF THE D_{s1} MESON

A. Matrix elements and decay widths

The matrix elements describing the strong $D_{s1} \rightarrow D_s^* \pi^0$ and radiative $D_{s1} \rightarrow D_s \gamma$ decays are defined as follows

$$M(D_{s1}^+(p) \rightarrow D_s^*(p') \pi^0(q)) = \epsilon_\mu(p) \epsilon_\nu^*(p') (g^{\mu\nu} G_{D_{s1} D_s^* \pi} - v'^\mu v^\nu F_{D_{s1} D_s^* \pi}) \quad (18)$$

and

$$M(D_{s1}^+(p) \rightarrow D_s(p') \gamma(q)) = \epsilon_\mu(p) \epsilon_\nu^*(q) (g^{\mu\nu} p q - q^\mu p^\nu) e G_{D_{s1} D_s \gamma}, \quad (19)$$

where $v = p/m_{D_{s1}}$ and $v' = p'/m_{D_s^*}$ are the four-velocities of the D_{s1} and D_s^* mesons, $G(F)_{D_{s1} D_s^* \pi}$ and $G_{D_{s1} D_s \gamma}$ are the corresponding effective coupling constants. The coherent sum of all the diagrams in Fig.3 contributing to the radiative decay $D_{s1} \rightarrow D_s \gamma$ is gauge invariant, while the contribution of each diagram is definitely not gauge invariant. As in Ref. [24], for convenience we split each individual diagram into a gauge-invariant piece and a remainder proportional to the Lorentz structure $g_{\mu\nu}$, which is noninvariant. One can prove that the sum of the noninvariant terms vanishes due to gauge invariance. In the following discussion of the numerical results we will only deal with the gauge-invariant contribution of the separate diagrams of Fig.3.

Using Eqs. (18) and (19) the strong $D_{s1} \rightarrow D_s^* \pi^0$ and radiative $D_{s1} \rightarrow D_s \gamma$ decay widths are calculated according to the expressions:

$$\begin{aligned} \Gamma(D_{s1} \rightarrow D_s^* \pi) &= \frac{P_{\pi^0}^*}{12\pi m_{D_{s1}}^2} \left\{ G_{D_{s1} D_s^* \pi}^2 + \frac{1}{2} \left(G_{D_{s1} D_s^* \pi} w - F_{D_{s1} D_s^* \pi} (w^2 - 1) \right)^2 \right\}, \\ \Gamma(D_{s1} \rightarrow D_s \gamma) &= \frac{\alpha}{3} G_{D_{s1} D_s \gamma}^2 P_\gamma^{*3} \end{aligned} \quad (20)$$

where $w = vv' = (m_{D_{s1}}^2 + m_{D_s^*}^2 - m_\pi^2)/(2m_{D_{s1}} m_{D_s^*})$; $P_{\pi^0}^* = \lambda^{1/2}(m_{D_{s1}}^2, m_{D_s^*}^2, m_{\pi^0}^2)/(2m_{D_{s1}})$ and $P_\gamma^* = (m_{D_{s1}}^2 - m_{D_s}^2)/(2m_{D_{s1}})$ are the corresponding three-momenta of the decay products with $\lambda(x, y, z) = x^2 + y^2 + z^2 - 2xy - 2xz - 2yz$ being the Källén function.

B. Numerical results

First we discuss the results for the strong decay $D_{s1} \rightarrow D_s^* \pi^0$. Here the main contribution to the decay width comes from the diagrams of Figs.2(c) and 2(d), while the contribution of the diagrams of Figs.2(a) and 2(b) is relatively suppressed by a factor of $\sim 10^{-2}$. On the other hand, the contribution to the decay width generated by the dominant coupling (proportional to $\cos \varepsilon$) exceeds the contribution due to the suppressed coupling (proportional to $\sin \varepsilon$) by a factor of 2 on average [see Lagrangian (12) and discussion in Sec.II]. The ‘‘dominant’’ coupling corresponds to the ‘‘direct’’ diagrams of Fig.2 in [24], while the second coupling concerns the ‘‘mixing’’ diagrams of Fig.3 in [24]. In this paper, we combine these two types of diagrams together using the unitary transformation (8).

In terms of the unknown dimensionless coupling constant $g_{D_s^* D^* K^*}$ the results for $\Gamma(D_{s1} \rightarrow D_s^* \pi)$ range from $(14.8 g_{D_s^* D^* K^*}^2)$ keV at $\Lambda_{D_{s1}} = 1$ GeV to $(23.4 g_{D_s^* D^* K^*}^2)$ keV at $\Lambda_{D_{s1}} = 2$ GeV. Choosing a typical value of $g_{D_s^* D^* K^*} \simeq g_{D_s^* D K} = 1.84$, we get

$$\Gamma(D_{s1} \rightarrow D_s^* \pi) = 50.1 - 79.2 \text{ keV} \quad (21)$$

where the range of values for our results is due to the variation of $\Lambda_{D_{s1}}$ from 1 to 2 GeV. An increase of $\Lambda_{D_{s1}}$ leads to an increase of the width. In Table 1 we present our results for the decay width $\Gamma(D_{s1} \rightarrow D_s^* \pi)$ including a variation of the scale parameter $\Lambda_{D_{s1}}$ from 1 to 2 GeV and compare them to previous theoretical predictions.

Now we turn to the discussion of the radiative decay $D_{s1} \rightarrow D_s \gamma$. By construction, using a gauge-invariant and Lorentz-covariant effective Lagrangian, the full amplitude for this process is gauge-invariant, while the separate contributions of the different diagrams of Fig.3 are not. It is important to stress that the diagrams of Fig.3 fall into two separately gauge-invariant sets: one set includes the diagrams of Figs.3(a), 3(c), 3(e), and 3(g) (with loops containing virtual D^{*+} and K^0 mesons), generated by the coupling of D_{s1} to the D^{*+} and K^0 constituents. Another set contains the diagrams of Figs.3(b), 3(d), 3(f), and 3(h) (with loops containing virtual D^{*0} and K^+ mesons) with the coupling of D_{s1} to D^{*0} and K^+ .

First we give the results for the effective coupling constant $G_{D_{s1} D_s \gamma}$: the total result and partial contributions of the different diagrams of Fig.3 (marked by 3(a), 3(b), etc.). In the analysis of the electromagnetic decay $D_{s1} \rightarrow D_s \gamma$

we restrict to the isospin limit, i.e. we do not include the isospin-breaking effects in the meson masses and proceed with the masses of the charged particles. In the isospin limit the diagrams of Fig.3(g) and 3(h) are equal to each other. For a value of $\Lambda_{D_{s1}} = 1$ GeV we get (here we only deal with the gauge-invariant parts of the diagrams of Figs.3(a)-3(d), 3(g), and 3(h), while the gauge-invariant parts of diagrams in Figs.3(e) and 3(f) are equal to zero):

$$\begin{aligned} G_{D_{s1}D_s\gamma} &= 0.106 \text{ GeV}^{-1}, & G_{D_{s1}D_s\gamma}^{3a} &= 0.008 \text{ GeV}^{-1}, & G_{D_{s1}D_s\gamma}^{3b} &= 0.090 \text{ GeV}^{-1}, \\ G_{D_{s1}D_s\gamma}^{3c} &= 7 \times 10^{-4} \text{ GeV}^{-1}, & G_{D_{s1}D_s\gamma}^{3d} &= -2 \times 10^{-4} \text{ GeV}^{-1}, & G_{D_{s1}D_s\gamma}^{3g} &\equiv G_{D_{s1}D_s\gamma}^{3h} = 0.004 \text{ GeV}^{-1}. \end{aligned} \quad (22)$$

From the results it is clear that the contact diagrams of Fig.3(c) and 3(d) are strongly suppressed, however these diagrams are kept to guarantee gauge invariance. The main contribution comes from the diagram of Fig.3(b) where the photon couples to the K^+ . Note, that the same conclusion concerning the dominance of the triangle diagram with the γK^+ coupling was obtained in the analysis of the radiative decay of the $D_{s0}^*(2317)$ into $D_s\gamma$ [24].

The result for the decay width of the transition $D_{s1} \rightarrow D_s\gamma$ is:

$$\Gamma(D_{s1} \rightarrow D_s\gamma) = 2.37 \text{ keV}. \quad (23)$$

In Table 2 we summarize our results for $\Gamma(D_{s1} \rightarrow D_s\gamma)$ including a variation of the scale parameter $\Lambda_{D_{s1}}$ from 1 to 2 GeV (an increase of $\Lambda_{D_{s1}}$ leads to a larger value for the width). We also compare to predictions of other theoretical approaches. Our results have a minor dependence on the parameter $\Lambda_{D_{s1}}$ and are also in agreement with previous calculations. Finally, in Table 3 we present a comparison of our results for the ratio $R = \Gamma(D_{s1} \rightarrow D_s\gamma)/\Gamma(D_{s1} \rightarrow D_s^*\pi)$ of the radiative and strong decay of D_{s1} mesons with data and other approaches. Our result for $R \simeq 0.05$ is insensitive to a variation of the size parameter $\Lambda_{D_{s1}}$.

IV. SUMMARY

We studied the new charm-strange meson $D_{s1}(2460)$ in the hadronic molecule interpretation, considering a bound state of D^* and K mesons. Using an effective Lagrangian approach we calculated the strong $D_{s1} \rightarrow D_s^*\pi^0$ and radiative $D_{s1} \rightarrow D_s\gamma$ decays. An important consequence of the D^*K molecular structure of the $D_{s1}(2460)$ meson is that the presence of $u(d)$ quarks in the D^* and K meson loops gives rise to a direct strong isospin-violating transition $D_{s1} \rightarrow D_s^*\pi^0$ in addition to the decay mechanism induced by $\eta - \pi^0$ mixing as was considered previously in literature. We found that the direct transition dominates over the $\eta - \pi^0$ mixing transition. In the present paper we combined these two mechanisms to the modified pion-emission diagrams due to the diagonalization of the pseudoscalar meson mass term [33] (see also Eq. (8)). In the language of the strong effective Lagrangian (12) the “direct” mechanism corresponds to the $KK^*\pi^0$ and $DD^*\pi^0$ couplings containing the $\tau_3 \cos \varepsilon$ flavor matrix, while the “mixing” mechanism corresponds to the $KK^*\pi^0$ and $DD^*\pi^0$ couplings containing the $I \cos \varepsilon$ flavor matrix. Finally, the main contribution to the strong decay $D_{s1} \rightarrow D_s^*\pi^0$ width arises from the diagrams of Figs.2(c) and 2(d). The contribution of the diagrams of Figs.2(a) and 2(b) to the decay width is suppressed by a factor of $\sim 10^{-2}$. In the case of the radiative decay $D_{s1} \rightarrow D_s\gamma$ the dominant contribution comes from the diagram of Fig.3(b).

Our results for the partial decay widths of the $D_{s1}(2460)$ and their ratio are summarized as follows:

$$\begin{aligned} \Gamma(D_{s1} \rightarrow D_s^*\pi) &= 50.1 - 79.2 \text{ keV}, \\ \Gamma(D_{s1} \rightarrow D_s\gamma) &= 2.37 - 3.73 \text{ keV}, \\ R &= \frac{\Gamma(D_{s1} \rightarrow D_s\gamma)}{\Gamma(D_{s1} \rightarrow D_s^*\pi)} \simeq 0.05. \end{aligned} \quad (24)$$

Acknowledgments

This work was supported by the DFG under contracts FA67/31-1 and GRK683. This research is also part of the EU Integrated Infrastructure Initiative Hadronphysics project under contract number RII3-CT-2004-506078 and President grant of Russia ”Scientific Schools” No. 5103.2006.2.

-
- [1] J. L. Rosner, Phys. Rev. D **74**, 076006 (2006) [arXiv:hep-ph/0608102].
- [2] T. Barnes, F. E. Close and H. J. Lipkin, Phys. Rev. D **68**, 054006 (2003) [arXiv:hep-ph/0305025].
- [3] B. Aubert *et al.* [BABAR Collaboration], Phys. Rev. Lett. **90**, 242001 (2003) [arXiv:hep-ex/0304021].
- [4] D. Besson *et al.* [CLEO Collaboration], Phys. Rev. D **68**, 032002 (2003) [arXiv:hep-ex/0305100].
- [5] K. Abe *et al.*, Phys. Rev. Lett. **92** (2004) 012002 [arXiv:hep-ex/0307052].
- [6] W. M. Yao *et al.* [Particle Data Group], J. Phys. G **33**, 1 (2006) and 2007 partial update for the 2008 edition.
- [7] P. Colangelo, F. De Fazio and R. Ferrandes, Mod. Phys. Lett. A **19**, 2083 (2004) [arXiv:hep-ph/0407137].
- [8] H. Y. Cheng and W. S. Hou, Phys. Lett. B **566**, 193 (2003) [arXiv:hep-ph/0305038].
- [9] W. A. Bardeen, E. J. Eichten and C. T. Hill, Phys. Rev. D **68**, 054024 (2003) [arXiv:hep-ph/0305049].
- [10] S. Godfrey, Phys. Lett. B **568**, 254 (2003) [arXiv:hep-ph/0305122].
- [11] P. Colangelo and F. De Fazio, Phys. Lett. B **570**, 180 (2003) [arXiv:hep-ph/0305140].
- [12] Fayyazuddin and Riazuddin, Phys. Rev. D **69**, 114008 (2004) [arXiv:hep-ph/0309283].
- [13] S. Ishida, M. Ishida, T. Komada, T. Maeda, M. Oda, K. Yamada and I. Yamauchi, AIP Conf. Proc. **717**, 716 (2004) [arXiv:hep-ph/0310061].
- [14] Y. I. Azimov and K. Goetze, Eur. Phys. J. A **21**, 501 (2004) [arXiv:hep-ph/0403082].
- [15] P. Colangelo, F. De Fazio and A. Ozpineci, Phys. Rev. D **72**, 074004 (2005) [arXiv:hep-ph/0505195].
- [16] F. E. Close and E. S. Swanson, Phys. Rev. D **72**, 094004 (2005) [arXiv:hep-ph/0505206].
- [17] W. Wei, P. Z. Huang and S. L. Zhu, Phys. Rev. D **73**, 034004 (2006) [arXiv:hep-ph/0510039].
- [18] A. Hayashigaki and K. Terasaki, Prog. Theor. Phys. **114**, 1191 (2005) [arXiv:hep-ph/0410393].
- [19] X. Liu, Y. M. Yu, S. M. Zhao and X. Q. Li, Eur. Phys. J. C **47**, 445 (2006) [arXiv:hep-ph/0601017].
- [20] J. Lu, X. L. Chen, W. Z. Deng and S. L. Zhu, Phys. Rev. D **73**, 054012 (2006) [arXiv:hep-ph/0602167].
- [21] F. K. Guo, P. N. Shen, H. C. Chiang and R. G. Ping, Phys. Lett. B **641**, 278 (2006) [arXiv:hep-ph/0603072].
- [22] F. K. Guo, P. N. Shen and H. C. Chiang, Phys. Lett. B **647**, 133 (2007) [arXiv:hep-ph/0610008].
- [23] Z. G. Wang, Phys. Rev. D **75**, 034013 (2007) [arXiv:hep-ph/0612225].
- [24] A. Faessler, T. Gutsche, V. E. Lyubovitskij and Y. L. Ma, Phys. Rev. D **76**, 014005 (2007) [arXiv:0705.0254 [hep-ph]].
- [25] D. Gamermann, L. R. Dai and E. Oset, Phys. Rev. C **76**, 055205 (2007) [arXiv:0709.2339 [hep-ph]].
- [26] D. Gamermann, Talk given at the 29th Course “Quarks in Hadrons and Nuclei”, September 16–24, 2007, Erice, Sicily.
- [27] M. F. M. Lutz, Talks given at the 11th International Conference on Meson-Nucleon Physics and the Structure of the Nucleon (MENU2007), September 10–14, 2007, Jülich, Germany and International School of Nuclear Physics, 29th Course “Quarks in Hadrons and Nuclei”, September 16–24, 2007, Erice, Sicily.
- [28] V. E. Lyubovitskij, Talks given at the 11th International Conference on Meson-Nucleon Physics and the Structure of the Nucleon (MENU2007), September 10–14, 2007, Jülich, Germany and International School of Nuclear Physics, 29th Course “Quarks in Hadrons and Nuclei”, September 16–24, 2007, Erice, Sicily.
- [29] A. Faessler, T. Gutsche, S. Kovalenko and V. E. Lyubovitskij, Phys. Rev. D **76**, 014003 (2007) [arXiv:0705.0892 [hep-ph]].
- [30] S. Weinberg, Phys. Rev. **130**, 776 (1963); A. Salam, Nuovo Cim. **25**, 224 (1962); K. Hayashi, M. Hirayama, T. Muta, N. Seto and T. Shirafuji, Fortsch. Phys. **15**, 625 (1967).
- [31] G. V. Efimov and M. A. Ivanov, *The Quark Confinement Model of Hadrons*, (IOP Publishing, Bristol & Philadelphia, 1993).
- [32] I. V. Anikin, M. A. Ivanov, N. B. Kulimanova and V. E. Lyubovitskij, Z. Phys. C **65**, 681 (1995); M. A. Ivanov, M. P. Locher and V. E. Lyubovitskij, Few Body Syst. **21**, 131 (1996); M. A. Ivanov, V. E. Lyubovitskij, J. G. Körner and P. Kroll, Phys. Rev. D **56**, 348 (1997) [arXiv:hep-ph/9612463]; M. A. Ivanov, J. G. Körner, V. E. Lyubovitskij and A. G. Rusetsky, Phys. Rev. D **60**, 094002 (1999) [arXiv:hep-ph/9904421]; A. Faessler, T. Gutsche, M. A. Ivanov, V. E. Lyubovitskij and P. Wang, Phys. Rev. D **68**, 014011 (2003) [arXiv:hep-ph/0304031]; A. Faessler, T. Gutsche, M. A. Ivanov, J. G. Körner, V. E. Lyubovitskij, D. Nicmorus and K. Pumsa-ard, Phys. Rev. D **73**, 094013 (2006) [arXiv:hep-ph/0602193]; A. Faessler, T. Gutsche, B. R. Holstein, V. E. Lyubovitskij, D. Nicmorus and K. Pumsa-ard, Phys. Rev. D **74**, 074010 (2006) [arXiv:hep-ph/0608015].
- [33] J. Gasser and H. Leutwyler, Nucl. Phys. B **250**, 465 (1985).
- [34] P. L. Cho and M. B. Wise, Phys. Rev. D **49**, 6228 (1994) [arXiv:hep-ph/9401301].
- [35] Z. G. Wang, J. Phys. G **34**, 753 (2007) [arXiv:hep-ph/0611271].
- [36] S. Mandelstam, Annals Phys. **19**, 1 (1962); J. Terning, Phys. Rev. D **44**, 887 (1991).

Table 1. Decay width of $D_{s1} \rightarrow D_s^* \pi^0$.

For our result the range of values is due to the variation of $\Lambda_{D_{s1}}$ from 1 to 2 GeV.

Approach	$\Gamma(D_{s1} \rightarrow D_s^* \pi^0)$ (keV)
Ref. [11]	7 ± 1
Ref. [10]	10
Ref. [22]	11.41
Ref. [9]	21.5
Ref. [12]	32
Ref. [20]	35
Ref. [17]	43 ± 8
Ref. [27]	140
Ref. [13]	155 ± 70
Ref. [14]	187 ± 73
Our result	50.1 – 79.2

Table 2. Decay width of $D_{s1} \rightarrow D_s \gamma$.

For our result the range of values is due to the variation of $\Lambda_{D_{s1}}$ from 1 to 2 GeV.

Approach	$\Gamma(D_{s1} \rightarrow D_s \gamma)$ (keV)
Ref. [19]	0.6 - 2.9
Ref. [14]	≈ 2
Ref. [9]	5.08
Ref. [23]	5.5 – 31.2
Ref. [10]	6.2
Ref. [16]	≤ 7.3
Ref. [15]	19 – 29
Ref. [27]	$\simeq 43.6$
Ref. [13]	93
Our result	2.37 – 3.73

Table 3. The ratio $R = \Gamma(D_{s1} \rightarrow D_s \gamma) / \Gamma(D_{s1} \rightarrow D_s^* \pi)$.

For our result the range of values is due to the variation of $\Lambda_{D_{s1}}$ from 1 to 2 GeV.

Approach	R
Ref. [14]	0.01 - 0.02
Ref. [9]	0.24
Ref. [27]	$\simeq 0.31$
Ref. [13]	0.41 - 1.09
Ref. [10]	0.62
Data [6]	0.44 ± 0.09
Our result	$\simeq 0.05$

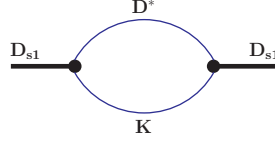


FIG. 1: Mass operator of the $D_{s1}(2460)$ meson.

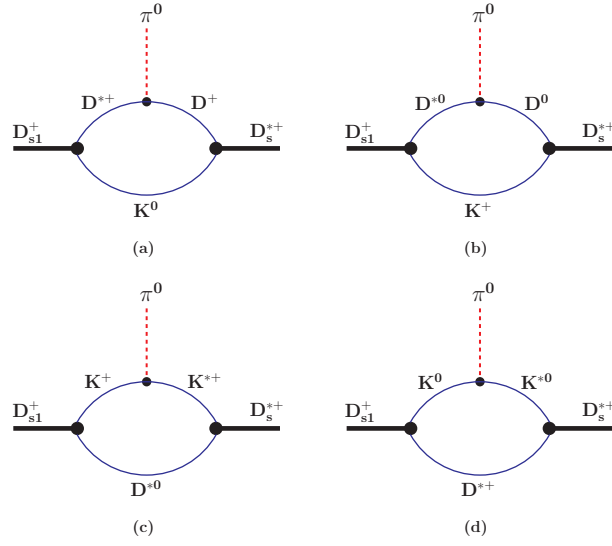


FIG. 2: Diagrams contributing to the strong transition $D_{s1}^+ \rightarrow D_s^{*+} + \pi^0$.

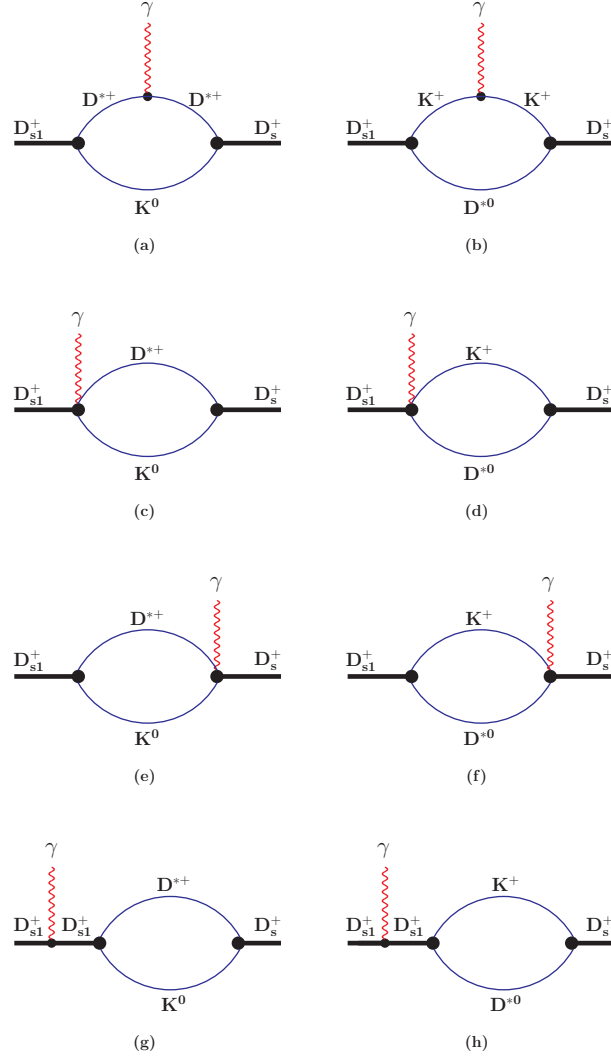


FIG. 3: Diagrams contributing to the radiative transition $D_{s1}^+ \rightarrow D_s^+ + \gamma$.